Development 138, 705-714 (2011) doi:10.1242/dev.055699

Specification of ion transport cells in the *Xenopus* larval skin

Ian K. Quigley, Jennifer L. Stubbs and Chris Kintner*

SUMMARY

Specialized epithelial cells in the amphibian skin play important roles in ion transport, but how they arise developmentally is largely unknown. Here we show that proton-secreting cells (PSCs) differentiate in the *X. laevis* larval skin soon after gastrulation, based on the expression of a 'kidney-specific' form of the H^+v-ATPase that localizes to the plasma membrane, orthologs of the Cl^-/HCO_3^- antiporters ae1 and pendrin, and two isoforms of carbonic anhydrase. Like PSCs in other species, we show that the expression of these genes is likely to be driven by an ortholog of foxi1, which is also sufficient to promote the formation of PSC precursors. Strikingly, the PSCs form in the skin as two distinct subtypes that resemble the alpha- and beta-intercalated cells of the kidney. The alpha-subtype expresses ae1 and localizes H^+v-ATPases to the apical plasma membrane, whereas the beta-subtype expresses pendrin and localizes the H^+v-ATPase cytosolically or basolaterally. These two subtypes are specified during early PSC differentiation by a binary switch that can be regulated by Notch signaling and by the expression of ubp1, a transcription factor of the grainyhead family. These results have implications for how PSCs are specified in vertebrates and become functionally heterogeneous.

KEY WORDS: Ionocyte, *Xenopus*, Epithelium, Kidney

INTRODUCTION

Transporting epithelia contain a diversity of specialized cell types, collectively called ionocytes, that mediate the selective secretion and adsorption of small molecules. Elucidating the mechanisms that generate this diversity and allow transporting epithelia to carry out their specific function remains an important goal in developmental biology. Toward this goal, recent work has focused on an epithelial cell type that drives the transepithelial movements of ions required for pH or osmoregulation by secreting protons across the plasma membrane using isoforms of the vacuolar-type H^+-transporting ATPase (H^+v-ATPase) (Brown and Breton, 1996). Proton-secreting cells (PSCs) are classically distinguished from other transporting epithelial cells based on their unusually high content of mitochondria, earning them the name mitochondria-rich cells (Brown and Breton, 1996; Hwang and Lee, 2007). More recently, they have been defined with PSC-specific gene expression, including cell-specific isoforms of the H^+v-ATPase such as *atp6v0a4* and *atp6v1b1*, anion antiporters used to exchange bicarbonate (HCO_3^-) for Cl^- such as slc26a4 (Pendrin), slc4a1 [anion exchanger 1 (ae1) or the Band 3 anion exchanger] and slc4a9 [anion exchanger 4 (ae4)], and carbonic anhydrases used to produce protons and HCO_3^- from water and carbon dioxide (Breton, 2001; Royaux et al., 2001; Wagner et al., 2009). PSCs are found in several mammalian organ systems, including the kidney, where they are termed intercalated cells (ICs) (Oliver, 1944; Wall, 2005), in the epididymis, where they are called clear or narrow cells (Brown and Breton, 1996), and in endolymphatic duct of the inner ear, where they are termed Deiter's or Claudius cells, or, collectively, FORE cells (Hulander et al., 2003). Disrupting the function of PSCs leads to several human diseases, including distal tubule acidosis, infertility and hearing loss (Hinton et al., 2009).

The Salk Institute for Biological Studies, 10010 North Torrey Pines Road, La Jolla, CA 92037, USA.

*Author for correspondence (kintner@salk.edu)

Accepted 12 December 2010

The development of PSCs in the mouse requires Foxi1, a member of the winged-helix family of transcription factors (Hulander et al., 2003; Blomqvist et al., 2004; Blomqvist et al., 2006). Mice mutant for *Foxi1* fail to form PSCs in the kidney, inner ear and epididymis, based on the loss of expression of PSC-specific subunits of the H^+v-ATPase and anion exchangers. Foxi1 directly regulates PSC genes involved in ion transport, based on the analysis of promoter fragments in transient transfection studies, suggesting that it acts as a crucial regulator of terminal PSC differentiation (Blomqvist et al., 2004; Vidarsson et al., 2009). Moreover, foxi1 is not only required to form PSCs in different mammalian organs, but also in other vertebrate species. In zebrafish, the *foxi1* orthologs *foxi3a* and *foxi3b* play overlapping roles in the differentiation of ionocytes that closely resemble PSCs in mammals (Hsiao et al., 2007; Janicke et al., 2007; Janicke et al., 2010). Studies of these cells in the zebrafish skin have also shown that their differentiation is negatively regulated by the Notch pathway, presaging findings that Notch also determines the number of ICs that form within the collecting duct of the mouse kidney (Jeong et al., 2009). In both cases, blocking Notch activity increases *foxi1* expression and the number of PSCs, whereas activating the Notch pathway inhibits *foxi1* expression and decreases PSC number. These studies suggest a model in which epithelial precursors require foxi1 to differentiate into PSCs and the number of precursors that express foxi1 is negatively regulated by the Notch pathway.

The differentiation of PSCs in the kidney is further complicated by the fact that several subtypes exist with different functional properties (Al-Awqati, 1996; Wall, 2005). The main subtypes are alpha-ICs, which reduce acidosis by secreting protons into the lumen of the collecting duct, and beta-ICs, which reduce alkalosis by secreting bicarbonate. To function as polar opposites during pH regulation, these two subtypes differentially localize the H^+v-ATPase along the apicobasal axis and differentially express the anion exchangers *Ae1* and *Pendrin* (Royaux et al., 2001; Devonald et al., 2003; Stehberger et al., 2003; Stehberger et al., 2007; Hinton et al., 2009). How different subtypes of ICs form has been mainly addressed in the mammalian adult, in which, under chronic pH

imbalances, the proportions of alpha- and beta-ICs appear to shift, leading to the suggestion that they are plastic and interconvertible (Al-Awqati, 1996; Schwartz et al., 2002; Wagner et al., 2002; Schwartz and Al-Awqati, 2005). This suggests that the differentiation of IC subtypes could rely on phenotypic plasticity; however, the mechanisms underlying IC subtype specification are largely unknown. The extracellular matrix molecule hensin/dmbt1 has been proposed to mediate subtype interconversion in pH shift experiments on cultured cells (Al-Awqati, 1996) and in vivo (Schwartz et al., 2002; Gao et al., 2010) but the transcriptional mechanisms underlying its activities are still unclear. Moreover, little is known about when ICs acquire subtype properties during their differentiation, or the developmental mechanisms that lead to the differential localization of the H^+v-ATPase or expression of *ae1* and *pendrin* during subtype specification (Hiatt et al., 2010).

Here, we examine the mechanisms that underlie the formation of different PSC subtypes by first describing the *Xenopus laevis* larval skin as a new model system for PSC differentiation. We show that PSCs form across the larval skin surface in a manner that is regulated by the Notch pathway and can be driven by foxi1. We show that PSCs form in the skin as at least two distinct subtypes that are remarkably similar to alpha- and beta-ICs in the kidney in terms of anion exchanger expression and H^+v-ATPase localization. We show that subtype-specific gene expression is already evident at PSC precursor stages, suggesting that subtype specification occurs developmentally during PSC differentiation. We shift the proportion of different subtypes by altering the levels of Notch activity, by misexpressing foxi1, or by altering the expression of the grainyhead-like transcription factor *ubp1*, which is normally expressed in the beta- but not alpha-subtype. In each experimental manipulation, the proportion of subtypes changes, but subtype identity is maintained as defined by ae1 expression, *pendrin* expression, and H^+v-ATPase localization. These results suggest that subtype identity is specified in PSC precursors by a binary switch that can be regulated by the Notch pathway and members of the grainyhead family.

MATERIALS AND METHODS

X. laevis fertilization, microinjection and embryo culture

Xenopus embryos were obtained by in vitro fertilization using standard protocols and maintained in 0.1× Marc's Modified Ringers (MMR) pH 7.4 (Sive et al., 1998). Embryos were injected at the 2- or 4-cell stage with capped synthetic mRNAs (1-5 ng) that encode the intracellular domain of Notch (ICD), a dominant-negative form of human mastermind HMM^{mut} (Wettstein et al., 1997; Fryer et al., 2002), or foxi1 or ubp1 cloned upstream of the human glucocorticoid receptor (Kolm and Sive, 1995). RNA encoding a membrane-localized mRFP or GFP was injected as a control or co-injected as a lineage tracer (Stubbs et al., 2006). Morpholinos (Gene Tools) directed against *atp6v1b1* RNA targeted the initiation codon (5′-GCCCCTCCACCCTCATTGCCACTTT-3′), and morpholinos directed against *ubp1* RNA targeted either the initiation codon (5′-GGTTG-GCTGTGCCAAAACAACATGT-3′) or a splice junction between exons 6 and 7 (5′-AAAGTAGGGAATGCACCTTAAAAAC-3′) (Heasman, 2002).

Transplant assays

The transplantation of outer layer ectoderm onto inner layer hosts was performed as described (Stubbs et al., 2006); in some cases, embryos were subsequently stained for immunofluorescence, as below.

In situ hybridization

Whole-mount in situ hybridizations were performed as described, omitting the proteinase K step and accompanying washes, using riboprobes generated from cDNAs (Harland, 1991). Two-color fluorescent in situ hybridization (FISH) was performed as described (Brend and Holley, 2009), omitting the methanol washes after development of TSA substrate. Embryos were then rinsed, mounted in PVA/DABCO (Sigma), and imaged on a BioRad Radiance 2100 confocal mounted to a Zeiss inverted microscope or a Zeiss LSM710, using a 25× or 63× objective. For cell counts, data were collected from at least three random fields (one field was equal to 196 μm^2 of the embryo surface) from at least five, but typically eight, embryos.

Immunofluorescence

X. laevis larvae were fixed for immunohistochemistry in fresh 4% paraformaldehyde in 0.8× phosphate-buffered saline (PBS) for 2 hours on ice followed by dehydration in 100% methanol. After rehydration, embryos were stained as described previously (Stubbs et al., 2006) in PBS containing 0.02% Tween 20 and 10% goat serum with the following primary antibodies: rabbit anti-ZO-1 (Zymed, 1:200), mouse anti-acetylated tubulin (Sigma, 1:200-1:1000), mouse anti-*Xenopus* E-cadherin (IDSHB clone 5D3, 1:500), monoclonal anti-AE1 (IDSHB clone IVF-12, 1:250), chicken anti-GFP (Aves, 1:500) or rabbit anti-atp6V1b1/2 (Santa Cruz, 1:100). Secondary antibodies comprised Cy2-, Cy3- or Cy5-labeled goat anti-IgG of the appropriate species (1:500, Jackson ImmunoResearch).

RNA isolation and microarray

Animal caps were explanted onto coverslips coated with fibronectin as described (Davidson et al., 2002). Total RNA was isolated using the proteinase K method from explanted ectoderm at the equivalent of stage 22-24 of development. Total RNA from explanted ectoderm was used to generate labeled complimentary RNA (cRNA) that was hybridized to *Xenopus laevis* l Genome Array chips (Affymetrix #900491). Microarray data were obtained from three independent experiments in which embryos were injected with *ICD* mRNA alone, or with HMM^{mut} mRNA. These data sets were analyzed using Bullfrog analysis software (Zapala et al., 2002), using a pairwise comparison, with the minimum fold change set at 3. Annotation of the dataset was then performed using Unigene identifiers. The complete microarray dataset has been submitted to the Gene Expression Omnibus (GEO; http://www.ncbi.nlm.nih.gov/geo/) under accession GSE23844.

Cloning of the *pendrin* promoter and transgenic methods

A PCR fragment was amplified from a *X. tropicalis* genomic library using one primer corresponding to the start of translation and the second located 3 kb upstream and shuttled into a vector containing the GFP coding region, followed by a short intron and poly(A) site from SV40. *X. laevis* transgenics were generated using the protocol of Kroll and Amaya (Amaya and Kroll, 1999) with modifications described by Sparrow et al. (Sparrow et al., 2000). Embryos generated by sperm nuclei injection were selected at the 4-cell stage for proper cleavage patterns and then injected with RNAs or morpholinos as indicated. Transgenic embryos were fixed without prior selection for GFP expression, stained with antibodies, and then scored under confocal microscopy. Transgenic embryos occurred at a frequency of 30-50% on average; quantitative data were collected by confocal microscopy as described above.

RESULTS

Blocking Notch in the developing skin of *X. laevis* embryos markedly increases two cell types that arise as precursors within the inner layer of the ectoderm and differentiate by moving into the outer epithelium (Stubbs et al., 2006). About half of these precursors give rise to multiciliate cells, whereas the other half give rise to a second cell type called intercalating non-ciliated cells (INCs) or small secretory cells (Stubbs et al., 2006; Hayes et al., 2007). INCs can be distinguished from other cell types in skin based on their morphology (Billett and Gould, 1971) and differential gene expression (Hayes et al., 2007), but their functional identity is unknown. To identify genes that are expressed at INC differentiation, we analyzed RNA isolated from cultured skin with decreased or increased Notch activity by hybridization to Affymetrix microarrays (see Materials and methods).

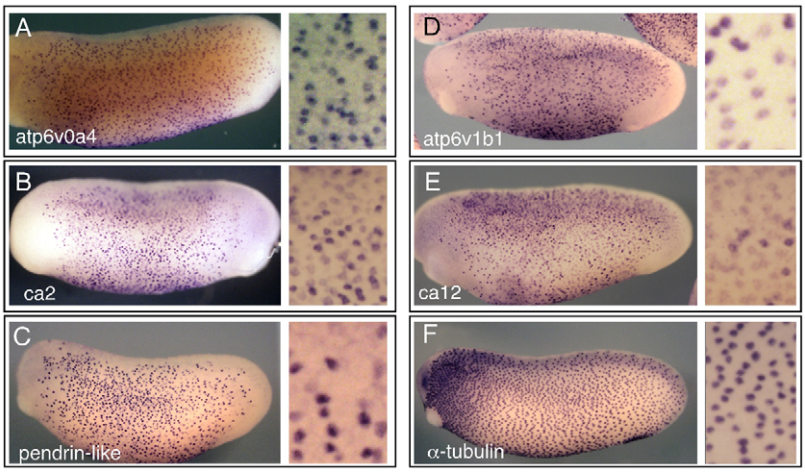

Fig. 1. Expression of ion transport genes in the *X. laevis* larval skin. Whole-mount in situ hybridization on stage 26 tadpoles was used to localize transcripts encoding proteins involved in ion transport, including (**A**,**D**) two subunits of the H^+v-ATPase, (**B**,**E**) two isoforms of carbonic anhydrase and (**C**) a pendrin-like anion exchanger. Note that these genes are expressed in scattered cells that are absent from the posterior and anterior areas of skin, in contrast to the pattern of ciliated cells marked by α-*tubulin* expression (**F**). A magnified view is shown in the neighboring panels.

Genes showing the largest fold change in this analysis (see Table S1 in the supplementary material) encode two transcription factors, foxi1 and ubp1, and proteins that are typically expressed by PSCs in other species. Four genes in the latter category encode isoforms of the H^+v-ATPase that localize to the plasma membrane, including *atp6v1c2* (112-fold change), *atp6v0a4* (100-fold change), *atp6v0d2* (55-fold change) and *atp6v1b1* (32-fold change) (Wagner et al., 2004; Pietrement et al., 2006; Kujala et al., 2007). Three genes on the list encode isoforms of carbonic anhydrase (ca): *ca2a* (64-fold change), *ca2b* (43-fold change) and *ca12* (81-fold change), enzymes that are highly expressed by PSCs in order to catalyze the production of H^+ and HCO_3^- from carbon dioxide and water (Breton, 2001). The list also contains an anion exchanger related to mammalian Pendrin, which exchanges HCO_3^- for Cl^- in some PSCs (Royaux et al., 2001; Hulander et al., 2003; Wall, 2005). Finally, another gene on the list encodes an unannotated member of the CLC family of chloride channels, genes also observed to be expressed in PSCs (Sakamoto et al., 1999; Kobayashi et al., 2001). As phylogenetic analysis of a subset of these genes suggested that they are direct orthologs of vertebrate genes implicated in PSC development and function (see Fig. S1 in the supplementary material), one possibility is that *X. laevis* skin contains a PSC that increases in number when Notch is blocked.

PSC-specific genes are expressed in an INC-like pattern in the skin

To determine which cells in the skin express the genes described above, we selected several representatives and characterized their expression in *X. laevis* larval embryos by whole-mount in situ hybridization (Fig. 1; see Figs S2 and S3 in the supplementary material). All genes tested, including *ca2*, *ca12*, *atp6v0a4*, *atp6v1b1*, *atp6v0d2*, *atp6v1e1*, *pendrin-like* and *pendrin*, gave a similar staining pattern, localizing to scattered cells throughout most of the skin but excluded from skin anterior to the eye and along the tailbud, a distribution that corresponds to the INCs/small secretory cells (Hayes et al., 2007) rather than ciliated cells. In addition, in contrast to the uniform expression of the ciliated cell marker α-*tubulin*, the expression of the ion transport genes varied in intensity from cell to cell, suggesting that the cells expressing these genes are a heterogeneous population (compare Fig. 1F with 1A-E), a possibility that is addressed further below. We also examined the expression of these genes in embryos in which Notch activity was inhibited or increased. As predicted, the number of cells expressing the PSC-specific genes increased markedly in embryos when Notch activity was inhibited (see Fig. S2 in the supplementary material) and decreased when Notch was overactive (Fig. 2G,H; data not shown). These data, along with the higher resolution localization studies described below, suggest that INCs are PSCs that form in the skin in a manner regulated by the Notch pathway.

foxi1-HGR induces the expression of ion transport genes

In other species, Foxi1 orthologs play a major role in the differentiation of PSCs (Hulander et al., 2003; Blomqvist et al., 2004; Blomqvist et al., 2006; Hsiao et al., 2007; Janicke et al., 2007; Vidarsson et al., 2009; Janicke et al., 2010). Thus, the finding that *X. laevis foxi1* (also called *Xema* or *foxi1e*) was the first gene on the list obtained from the array analysis described above is striking (see Table S1 in the supplementary material). Previous studies have shown that *X. laevis foxi1* is first expressed at blastula stages within the ectoderm, is required for germ layer specification (Suri et al., 2005; Mir et al., 2007), and then strongly expressed following gastrulation in scattered cells of the skin, in a manner regulated by Notch signaling (Mir et al., 2008) (see Fig. S3 in the supplementary material).

Based on these observations, one possibility is that *foxi1* first plays a role in ectoderm specification, but then later plays a role in specifying the differentiation of INCs as PSC-like cells, by regulating the expression of genes involved in ion transport. To test this idea, and to avoid possible ectodermal specification problems resulting from early misexpression, we fused the ligand-binding domain of the human glucocorticoid receptor to the C-terminus of *X. laevis* foxi1 (foxi1-HGR) (Kolm and Sive, 1995). Our reasoning was that foxi1-HGR could be expressed in embryos by RNA injection, stay in an inactive form during blastula stages when germ layer specification occurs, but could then be activated after gastrulation by adding the synthetic hormone dexamethasone (DEX).

Expression of the PSC-specific genes was dramatically upregulated in early tadpoles that were injected with *foxi1-HGR* mRNA at the 2-cell stage and treated with DEX at stage 12 (Fig. 2A,B; data not shown). No obvious changes in gene expression occurred without DEX treatment, indicating that they are caused by the late action of foxi1 (data not shown), presumably after its role in germ layer specification. Injecting *foxi1-HGR* had slightly inhibitory effects on the expression of the ciliated cell marker α-*tubulin* (Fig. 2C). Injecting embryos with mRNA encoding another forkhead

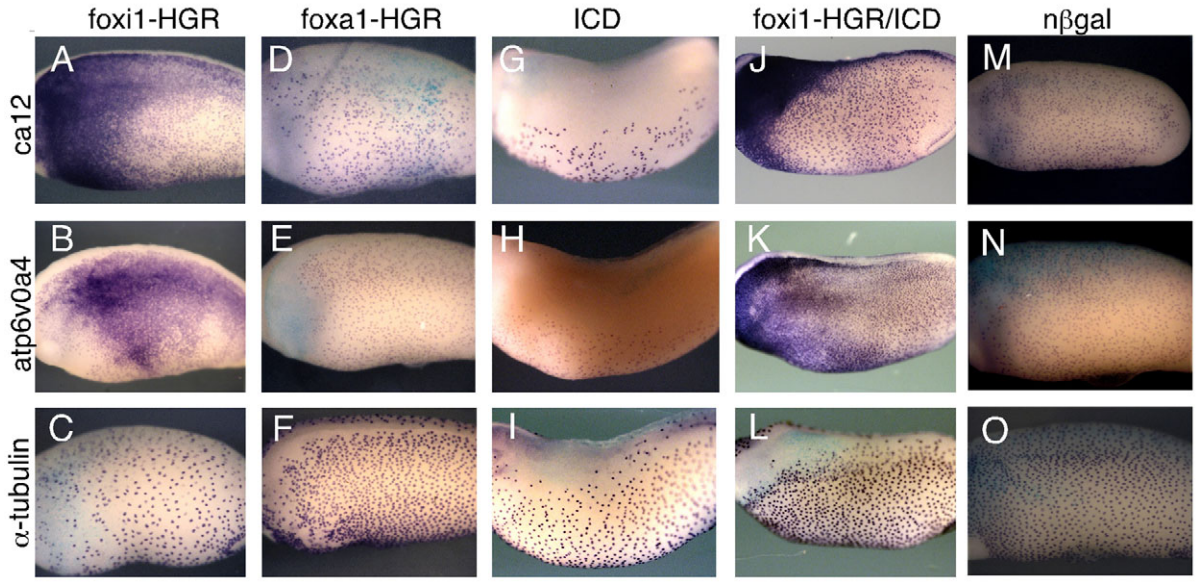

Fig. 2. foxi1-HGR strongly upregulates the expression of ionocyte genes. (**A-O**) *Xenopus* embryos were injected at the 2-cell stage with mRNAs encoding foxi1-HGR or foxa1-HGR, activated Notch (ICD) or with both foxi-HGR and ICD, treated with dexamethasone (DEX) at stage 12, fixed at stage 26 and stained for expression of the indicated genes by whole-mount in situ hybridization. foxi1-HGR, but not foxa1-HGR, strongly induced the ectopic expression of *ca12* (A) and *atp6V0A4* (B), even in the presence of ICD (J,K) but had no effect, or a slight inhibitory effect, on the expression of the ciliated cell marker α-*tubulin* (C). *n-lacZ* RNA injections (nβgal) served as a negative control (M-O).

transcription factor, foxa1, fused to HGR had no apparent effect on the expression of PSC-specific genes (Fig. 2D,E). Activated Notch blocks the formation of INCs (Stubbs et al., 2006), the expression of the ion transport genes (Fig. 2G,H), as well as the expression of *foxi1* (Mir et al., 2008). However, foxi1-HGR also induced PSC-specific gene expression in the presence of activated Notch (ICD), suggesting that foxi1 acts downstream of Notch to activate gene expression required for PSC differentiation (Fig. 2J,K).

foxi1-HGR induces cell intercalation

foxi1-HGR might simply induce ectopic expression of PSC-specific genes, or, alternatively, it might induce the formation of ectopic INCs. To distinguish between these two possibilities, we assayed the morphology of the skin in embryos injected with *foxi1-HGR* at the 2-cell stage and treated with DEX at stage 12. At stage 26, the morphology of the skin in *foxi1-HGR*-injected, DEX-treated larvae differed markedly from control larvae in two respects (Fig. 3B versus 3A). First, *foxi1-HGR*/Dex induced a 3- to 4-fold increase in the number of cells with an INC morphology (Fig. 3B,E). Second, ciliated cells (CCs) still appeared in the *foxi1-HGR*-expressing embryos based on acetylated tubulin staining and their characteristic morphology, but many failed to form cilia (Fig. 3B,E). These aberrant CCs formed in increased numbers but this could be a consequence of disabling the Notch pathway (Stubbs et al., 2006). To test this idea, we expressed the activated form of Notch, ICD, in skin at levels that normally block the appearance of both CCs and INCs (Fig. 3C,E; see Fig. S4A-C,G in the supplementary material). In skin that expressed both ICD and foxi1-HGR and was then treated with DEX, the aberrant CCs were absent but INCs still appeared in increased numbers (Fig. 3D,E), suggesting that foxi-HGR acts downstream of Notch to promote the formation of PSCs but not CCs. Using a transplant assay to distinguish between skin cells derived from the two layers (Stubbs et al., 2006), we found that the number of intercalating inner cells increased markedly in response to foxi1-HGR, and this occurred even in the presence of ICD, which normally blocks intercalation

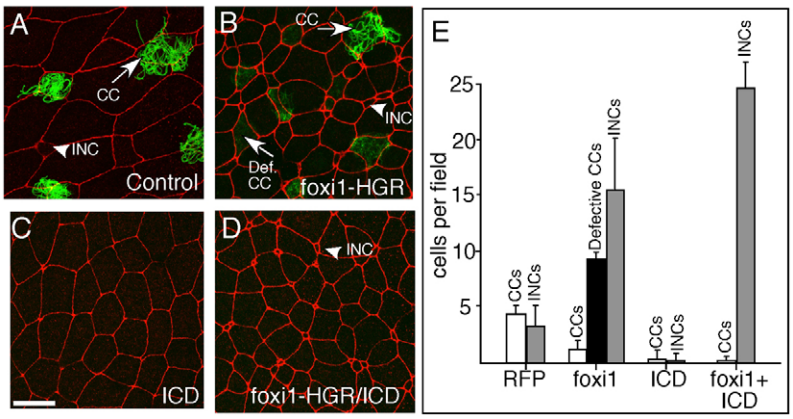

Fig. 3. foxi1-HGR promotes INC formation. (**A-D**) Two-cell *Xenopus* embryos were injected with RNA encoding foxi1-HGR and ICD along with *mRFP* RNA as a tracer, treated with DEX at stage 12, fixed at stage 26, and stained with anti-acetylated tubulin (green) to identify ciliated cells (CCs). Shown is a confocal image of the skin in embryos injected with just *RFP* (A), *foxi1-HGR* (B), *ICD* (C) or with both *foxi1-HGR* and *ICD* RNA (D). (**E**) Quantification of different cell types in the skin under the indicated experimental conditions. CCs stained with the acetylated tubulin antibody (green) were classified as defective if they failed to form cilia. INCs and outer cells (OCs) were scored based on their characteristic small and large apical domain, respectively. Error bars indicate + s.d. All values are significantly different relative to the control, based on a two-tailed *t*-test ($P \leq 0.005$). Scale bar: 20 μm.

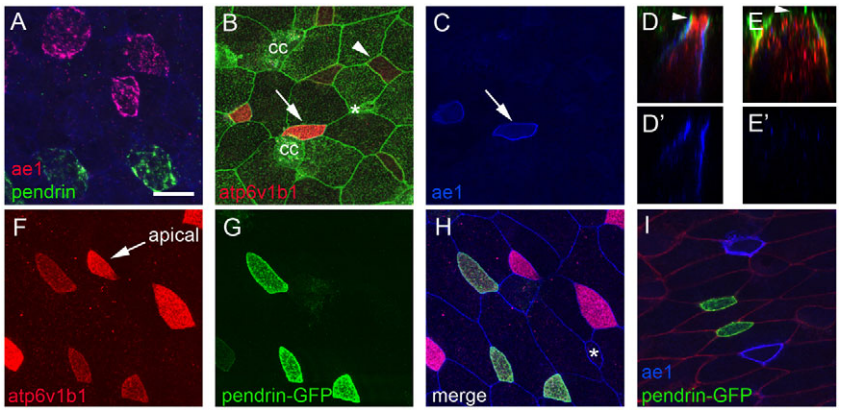

Fig. 4. INC subtypes. (**A**) Analysis of *Xenopus* larval skin at stage 26 using two-label FISH probes for ae1 (red) and pendrin (green) identifies two approximately equal populations of INCs. (**B-E′**) Embryo injected at the 2-cell stage with *mGFP* RNA was fixed and stained at stage 26 with B1 (red) and ae1 (blue) antibodies. Note that INCs with strong apical B1 staining (B, arrow) also stain with ae1 (C, arrow) whereas those with basolateral B1 staining (B, arrowhead) do not. *z*-section through cells with apical B1 staining (compare arrowheads in D and E) shows that ae1 localizes basolaterally (D,D′), whereas in cells with cytosolic or basolateral B1 staining ae1 is absent (E,E′). (**F-H**) *pendrin-GFP^{tr}* embryos were fixed at stage 26 and stained with antibodies to B1 (red) and E-cadherin (blue). Shown is B1 staining (F), GFP expression (G), or a merge of all three channels (H). (**I**) *pendrin-GFP^{tr}* embryos were injected with *mRFP* RNA (red) to label cell boundaries and stained with ae1 antibody (blue). CC, ciliated cell. Asterisk marks a small population of INCs that do not stain with or express ae1, pendrin or B1. Scale bar: 20 μm.

(see Fig. S4D-G in the supplementary material) (Stubbs et al., 2006). Thus, foxi1-HGR can act downstream of Notch to generate precursors that intercalate into the outer cell layer and presumably go on to differentiate into PSCs.

INCs fall into two subtypes

The isoforms of the H$^+$v-ATPase expressed by INCs have been shown to localize to the plasma membrane in PSCs in other species (Wagner et al., 2004; Pietrement et al., 2006; Hinton et al., 2009). To determine whether this holds true in *Xenopus* INCs, we examined the localization of the H$^+$v-ATPases using an antibody raised against a peptide conserved in both the atp6v1b1 and b2 subunits. To test antibody specificity, we also stained embryos injected with a morpholino designed to block the expression of atp6v1b1 but not closely related *X. laevis* subunits (e.g. atp6v1b2). In wild-type embryos, the antibody strongly stained the plasma membrane of INCs but not outer cells or CCs (Fig. 4; see Fig. S5B,C in the supplementary material), whereas in atp6v1b1 morphants this staining was lost (see Fig. S5E,F in the supplementary material). We conclude that the major epitope detected in INCs with the B1 antibody is atp6v1b1 and that the H$^+$v-ATPase localizes to the plasma membrane in INCs as in other PSCs.

Strikingly, one population of INCs showed strong apical staining with the B1 antibody, whereas in the other population staining was more basolateral or cytoplasmic, in a manner that mirrored the differential localization of the H$^+$v-ATPase in alpha- and beta-ICs in the kidney (compare Fig. 4D with 4E and see also 4B,F; see Fig. S5B in the supplementary material).

To pursue this finding further, we examined the *X. laevis* homologs of *ae1* and *pendrin*, as expression of these genes in the kidney differentially marks alpha- and beta-ICs, respectively (Royaux et al., 2001) (see Fig. S3K-Y in the supplementary material). Using two-label FISH and confocal microscopy, we found that *pendrin* and *ae1* mRNAs localize to non-overlapping, but roughly equal, populations of INCs, in contrast to the INC-wide expression of RNAs encoding foxi1 or subunits of the H$^+$v-ATPase (Fig. 4A; see Fig. S3A-J in the supplementary material; data not shown). Similar expression of ae1 was also detected in about half the INCs using a monoclonal antibody raised against human AE1 (Fig. 4C-E,I). ae1 staining localized to the basolateral plasma membrane (Fig. 4C,D′,I), and the INCs that stained for ae1 were the same as those that showed strong apical staining with the B1 antibody (compare Fig. 4B with 4C and 4D with 4D′), as found for alpha-ICs in the kidney.

Finally, because we were unable to identify an antibody that recognizes *X. laevis* pendrin, we took a transgenic approach to mark *pendrin*-expressing cells. A 3.0 kb fragment proximal to the start of transcription of the *X. tropicalis pendrin* gene was isolated by PCR, cloned upstream of sequences encoding a membrane-localized form of eGFP, and introduced into *X. laevis* embryos using the sperm nuclei transfer method (Amaya and Kroll, 1999). In *pendrin-GFP* transgenic (*pendrin-GFP^{tr}*) larvae, GFP expression was detected in INCs but not outer cells or CCs (Fig. 4G-I; see Fig. S5 in the supplementary material). Moreover, GFP expression occurred in INCs with basolateral B1 staining, and was absent in INCs that express ae1 (Fig. 4F-I), as found for beta-ICs in the kidney.

Together, these results show that INCs fall into two subtypes based on the localization of the H$^+$v-ATPase and the differential expression of *ae1* and *pendrin*. By analogy with ICs in the kidney, we refer hereafter to INCs with *ae1* expression and apical H$^+$v-ATPase localization as the alpha-subtype, and those with *pendrin* expression and basolateral H$^+$ v-ATPase localization as the beta-subtype.

Subtype specification occurs during early INC differentiation

Since the timing of IC subtype specification during development has not yet been extensively examined in the mouse, we determined when subtype identity first arises during PSC differentiation in *Xenopus* by assaying the developmental expression of *foxi1*, *atpv0a4*, *ae1* and *pendrin* (see Fig. S3 in the supplementary material). As shown previously, spotty expression of *foxi1* in the developing skin suggested that INCs initiate differentiation during gastrulation (see Fig. S3 in the supplementary

material) (Suri et al., 2005; Mir et al., 2007). Soon after gastrulation was complete, expression of *atpv0a4* was detected in a spotty pattern at stage 13, marking the early phase of PSC differentiation (see Fig. S3F in the supplementary material). Significantly, at the same time as *atpv0a4* expression began, *pendrin* expression was also detected in a subset of INCs (see Fig. S3K in the supplementary material). *ae1* expression first occurred slightly later, at stage 15, but still before INCs had completed radial intercalation (see Fig. S3U in the supplementary material) (Stubbs et al., 2006). Thus, based on *ae1* and *pendrin* expression, INC precursors exist as different subtypes prior to terminal differentiation, suggesting that subtype specification involves developmental mechanisms that operate during PSC formation rather than as a direct response to physiological conditions.

Notch signaling regulates INC subtype specification

The two INC subtypes form in the skin in approximately equal numbers, and are intermingled across the skin, suggesting that they might be specified via local cell-cell interactions. One possibility, therefore, is that Notch signaling is used again in the PSC lineage to influence the formation of different subtypes. To test this possibility, we examined INC subtype formation in embryos in which Notch activity was inhibited using a dominant-negative form of mastermind, or increased by injecting limiting amounts of ICD. Both INC subtypes increased in number when Notch was disabled, but the beta-INCs formed proportionally at much higher levels than alpha-INCs, suggesting that loss of Notch favors beta-INC formation (Fig. 5). Conversely, in embryos injected with limiting amounts of ICD, the formation of alpha-INCs was dramatically favored over that of beta-INCs (Fig. 5). Thus, Notch signaling contributes to the specification of INC subtypes, presumably by regulating the expression of factors involved in beta-INC and alpha-INC formation.

ubp1 marks and influences INC subtype specification

Disabling Notch in the skin also leads to marked increases in the expression of a second transcription factor gene that is annotated as *ubp1* in Xenbase, but is the closest ortholog to *lbp1a* in higher vertebrates (see Table S1 and Figs S1 and S6 in the supplementary material). *ubp1*, along with *cp2* and *cp2l1*, define a subfamily of the grainyhead transcription factors conserved in vertebrates (Yoon et al., 1994; Wilanowski et al., 2002; Katsura et al., 2009). In the mouse, a targeted mutation in *Ubp1* leads to defects in extraembryonic tissues that has thus far precluded an analysis of *Ubp1* function during embryogenesis (Parekh et al., 2004). Accordingly, we examined the role of *ubp1* in *Xenopus* skin, analyzing its expression by in situ hybridization. *ubp1* was expressed in a spotty pattern in the skin in the same manner as other INC markers (see Fig. S3Z-DD in the supplementary material), and blocking Notch led to a dramatic increase in cells expressing *ubp1*, whereas activating Notch led to a reduction (see Fig. S7A-D in the supplementary material). Using FISH and confocal microscopy, *ubp1* expression was seen to localize to the *pendrin*-expressing beta-INCs, but was either absent or strongly reduced in *ae1*-expressing alpha-INCs (Fig. 6A,B), making *ubp1* the first known transcription factor that marks a specific PSC subtype. Therefore, its subtype-specific expression and its regulation by Notch suggest a potential role for *ubp1* in beta-INC formation.

We next examined the role of ubp1 in subtype specification by expressing in embryos a form of ubp1 fused to HGR. When not treated with DEX, the numbers of alpha- or beta-INCs were

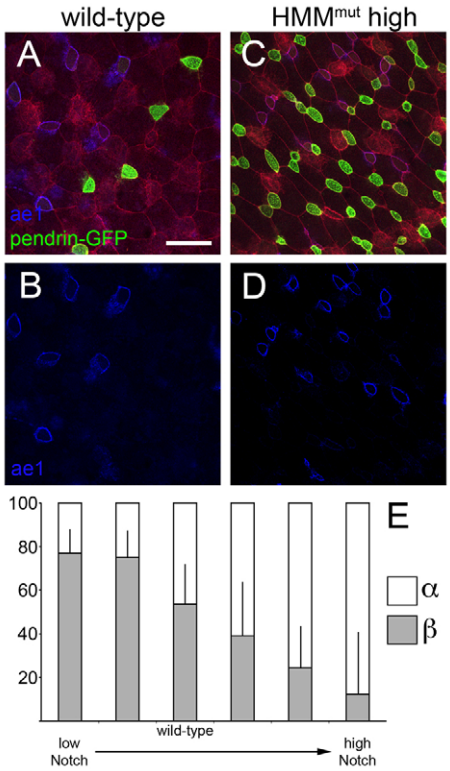

Fig. 5. Notch signaling directs INC subtype specification. (**A**,**B**) Wild-type distribution of alpha- and beta-INCs. (**C**,**D**) High doses of *HMM*^{mut} mRNA increase both INC subtypes, but favor beta-INC differentiation, as determined by ae1 and pendrin-GFP staining or by atp6v1b1 localization (not shown). (**E**) Notch signaling was titrated either with two decreasing doses of HMM^{mut} to block signaling or three increasing doses of ICD to promote signaling, and then embryos were assayed for proportions of alpha- and beta-subtypes by confocal microscopy and cell counting. Cells were counted from at least three confocal fields from several embryos, typically eight. Raw INC subtype numbers were then converted into percentages and arcsine transformed. Two-tailed *t*-tests indicated significant differences between each dose ($P \leq 0.05$) except for the two HMM^{mut} doses, which were not significantly different (the two leftmost columns). Error bars indicate + s.d. Scale bar: 40 μm.

unchanged in injected embryos based on B1 localization and ae1 expression (see Fig. S8 in the supplementary material). Strikingly, activation of ubp1-HGR with DEX at stage 12 inhibited the formation of alpha-INCs while inducing additional beta-INCs, as marked by whole-mount *ae1* and *pendrin* RNA expression (see Fig. S7E-H in the supplementary material), by detection of *ae1* and *pendrin* RNA using FISH (Fig. 6C), or by ae1 antibody staining of *pendrin-GFP* transgenics (Fig. 6D). Quantification of the different INC subtypes in ubp1-HGR-injected embryos indicated that *ubp1* misexpression not only biases subtype specification toward beta-INCs but also increases the total INC number.

We also examined H^+v-ATPase localization in INCs in ubp1-HGR-injected embryos, and found a similar reduction of apical localization indicative of alpha-INCs and an increase in basolateral localization indicative of beta-INCs (Fig. 6E). We did not observe any cells co-expressing *pendrin* and *ae1* by transcript, transgene or protein, nor did we see ae1-positive cells with basolateral atp6v1b1 or ae1-negative cells with apical atp6v1b1 (not shown), suggesting

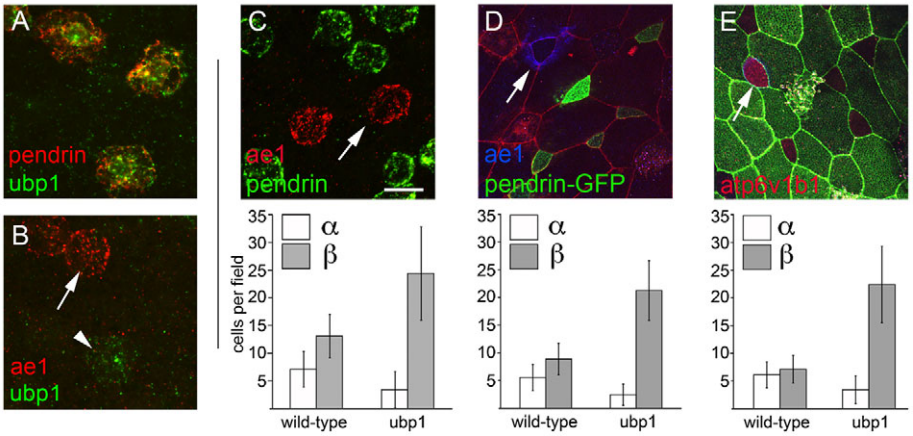

Fig. 6. ubp1 regulates beta-INC specification. (**A**,**B**) Two-color FISH indicates that *ubp1* is co-expressed with *pendrin*, which marks beta-INCs (A), but not with *ae1*, a marker of alpha-INCs (B). The arrow marks an *ae1*-expressing cell and the arrowhead marks a *ubp1*-expressing cell. (**C-E**) *Xenopus* embryos were injected with *ubp1-HGR* RNA at the 2-cell stage, treated with DEX at stage 12 and then fixed at stage 26 to quantify the number of alpha-INCs and beta-INCs using three different approaches: two-label FISH for *ae1* (red) and *pendrin* (green) mRNA (C); *pendrin-GFP*^{tr} transgenics (green) with ae1 antibody staining (blue) and mRFP (red) (D); or mGFP (green) and B1 antibody staining (red) (E). Arrows mark alpha-INCs. Cells were counted from at least three random fields (196 μm^2 of embryo surface) from at least five embryos, typically eight; fields shown are 98 μm^2. Error bars indicate ± s.d. All values between a given INC subtype under various conditions are significantly different relative to the control, based on a two-tailed *t*-test ($P \leq 0.005$). Scale bar: 20 μm.

that the alpha-INC and beta-INC identities remained intact under these manipulations. Finally, we induced ubp1-HGR-injected embryos with DEX at both stage 12, when INC precursors first form, and at stage 18, when INCs have differentiated, and scored subtype identity at stage 26 (see Fig. S8 in the supplementary material). Misexpressing ubp1 suppressed alpha-INC subtype formation at stage 12 but not at stage 18, suggesting that once alpha-INCs have formed they cannot be interconverted to a beta fate by ubp1 activity.

ubp1 acts downstream of foxi1 to suppress alpha-INC differentiation

ubp1 could conceivably influence INC subtype specification by altering the ability of foxi1 to activate gene expression in the subtype lineages. To test this possibility, we examined INC subtype specification at stage 26 in embryos injected with *foxi1-HGR* RNA and treated with DEX at stage 12. By whole-mount in situ hybridization, foxi1-HGR strongly increased the number of cells expressing *ae1*, suggesting that the INCs induced by ectopic foxi1 were primarily alpha in character (see Fig. S9A-B in the supplementary material). By contrast, foxi1-HGR produced a much more modest increase in the number of cells expressing *pendrin*, as determined by whole-mount in situ hybridization (see Fig. S9C-D in the supplementary material) and confirmed when foxi1-HGR was expressed in *pendrin-GFP* transgenics (data not shown). However, when assayed by ae1 antibody staining to quantify this result, foxi1-HGR strongly induced ae1 ectopically in outer cells, thus obscuring whether the INCs induced by foxi1-HGR were ae1 positive or negative (Fig. 7D). To circumvent this problem, we used a transplantation assay (see Fig. S9G in the supplementary material) to restrict foxi1-HGR expression to the inner layer cells. This assay confirmed that the majority of INCs induced by foxi1-HGR were ae1 positive, with a much more modest increase in ae1-negative INCs, similar to that seen when scored by *pendrin* expression (see Fig. S9E-J in the supplementary material). Thus, the increase in INC formation produced by foxi1-HGR biases the generation of alpha- over beta-INCs (see Fig. S9 in the supplementary material).

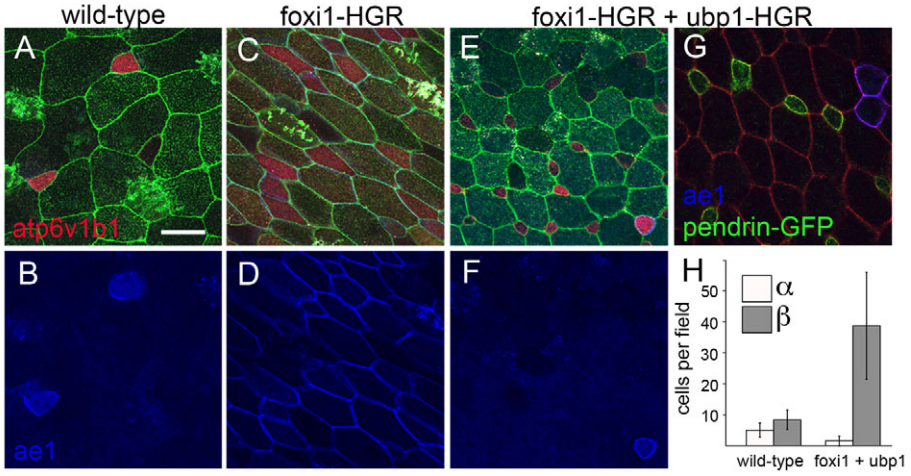

Fig. 7. ubp1-HGR converts foxi1-HGR-induced alpha-INCs into beta-INCs. (**A-F**) *Xenopus* embryos were injected at the 2-cell stage with *foxi1-HGR* or with both *foxi1-HGR* and *ubp1-HGR* RNA, along with *mGFP* RNA as a tracer. Injected embryos were treated with DEX at stage 12, fixed at stage 26, and then stained with B1 (red, upper panels) and with ae1 (blue, lower panels) antibodies. (**G**) *pendrin-GFP*^{tr} embryos were injected with *foxi1-HGR*, *ubp1-HGR* and *mGFP* as tracer, and then stained with ae1 antibody (blue). (**H**) Based on ae1 and B1 staining, alpha-INCs and beta-INCs per field were scored under the various conditions; each field represents 196 μm^2 of embryo surface. Error bars indicate ± s.d. Scale bar: 20 μm.

To determine whether ubp1 can influence the subtypes of INCs induced by foxi1-HGR, embryos were injected with both *ubp1-HGR* and *foxi1-HGR* mRNA and treated with DEX at stage 12. In these embryos, ae1 expression in the outer layer cells was largely repressed, and most of the INCs now differentiated as beta-INCs rather than alpha-INCs, based on antibody staining against ae1 and atp6v1b1 as well as *pendrin-GFP* expression (Fig. 7E-G). Thus, foxi1 on its own appears to tip the balance toward alpha-INC specification, whereas ubp1 can tip the balance back to beta-INC specification.

DISCUSSION

The adult frog skin has been extensively studied as a transporting epithelium, reflecting the fact that it mediates both NaCl uptake under low ionic conditions and pH homeostasis (Schachowa, 1876; Schulze, 1876; Schiefferdecker, 1881; Krogh, 1937; Krogh, 1938). These studies have identified cells that have been proposed to be analogous to ICs in the kidney, based on the fact that they independently exchange Na^+ for H^+ and Cl^- for HCO_3^- (Larsen et al., 1996; Ehrenfeld and Klein, 1997; Jensen et al., 2003), using a proton-motive force attributed to a H^+v-ATPase pump related to that in mammalian ICs (Klein et al., 1997; Jensen et al., 2002). Here, we provide evidence that cells remarkably similar to the ICs of the mammalian kidney arise in the *Xenopus* larval skin. We also show that these cells are likely to be functionally heterogeneous, resembling the two main subtypes of ICs (Royaux et al., 2001; Devonald et al., 2003; Jensen et al., 2003). Finally, we exploit this new model system to explore how PSCs become specified developmentally and heterogeneous in function.

Cell type specification in the skin

INCs express many of the genes that characterize PSCs in mammals, including the 'kidney-specific' subunits of the H^+v-ATPase, atp6v1b1 and atp6v0a4, which when mutated induce recessive distal renal tubular acidosis (dRTA) in humans (Karet et al., 1999; Stehberger et al., 2003; Breton and Brown, 2007). Like PSCs in mammals and fish (Hulander et al., 2003; Blomqvist et al., 2004; Blomqvist et al., 2006; Hsiao et al., 2007; Janicke et al., 2007; Vidarsson et al., 2009; Janicke et al., 2010), the expression of these genes in INCs appears to be driven by foxi1 (Vidarsson et al., 2009). The role of foxi1 in PSC differentiation, however, is likely to extend beyond the activation of genes that mediate the ion transport properties of PSCs. foxi1-HGR is also very potent at inducing cells to undergo radial intercalation, one of the first steps in the differentiation of PSCs in the skin and perhaps in other tissues as well. PSC precursors can already be distinguished from intercalating CC precursors based on differences in their morphogenetic behaviors during radial intercalation (Stubbs et al., 2006). That foxi1-HGR induces intercalating cells with PSC-like properties argues for a very early role for foxi1 in the generation of PSC precursors from uncommitted epithelial cells. The identification of genes that are activated by foxi1 in epithelial precursors might therefore provide insights into how PSCs acquire their unique morphological features, as well as how these cells carry out their physiological function.

INCs subtypes in the skin

INCs also fall into two subtypes that are directly analogous to the IC subtypes in the kidney. Beta-INCs express *pendrin* and localize the H^+v-ATPase basolaterally, whereas alpha-INCs express *ae1* and localize the H^+v-ATPase apically (Al-Awqati, 1996; Royaux et al., 2001; Kim et al., 2002; Devonald et al., 2003; Wall, 2005; Schulz et al., 2007). The two subtypes form in the skin in approximately equal numbers, are intermingled across the skin, but show some degree of clustering (see Fig. S3 in the supplementary material; data not shown). This pattern argues against a strong regional patterning signal or a strict lineage mechanism that leads to subset diversification. Moreover, a developmental series shows that *pendrin* is already expressed in PSC precursors as they undergo intercalation, with *ae1* expression following soon thereafter, suggesting that PSCs differentiate as distinct subtypes (see Fig. S3 in the supplementary material) (see also Song et al., 2007). As these developing PSC subtypes have yet to encounter the external environment, it is unlikely that they are first generated in the skin as generic or mixed subtypes that only resolve into the two polar opposites based on physiological conditions. Rather, subtype specification is likely to be initiated by genetic pathways operating in precursor cells. This conclusion does not preclude the possibility that, at later stages, PSCs are indeed plastic and interconvert between beta-INCs and alpha-INCs, as has been proposed for ICs in the kidney.

Transcriptional control of subtype specification

The developmental specification of subtypes occurs, therefore, during PSC differentiation, when foxi1 appears to activate not only those genes required in all PSCs, but also those expressed in a subtype-specific manner. Thus, one model is that additional transcription factors are required in PSCs to suppress alpha gene expression in betas and vice versa during subtype specification, resulting in a binary switch. Results obtained from experiments in which we manipulated ubp1, the Notch pathway and foxi1 provide support for the idea that subtype specification is driven by a transcriptional network acting in the INC precursors in the manner suggested by this model.

We show here that blocking Notch also has a profound effect on the formation of INC subtypes, in that both subtypes increase in number but with betas increasing proportionally much more than alphas. Conversely, expressing limiting amounts of activated Notch in the skin leads to a situation in which INC precursors primarily become alpha-INCs. These data strongly suggest that the level of Notch activity in INC precursors is one factor that can influence subtype specification, and it will be interesting to determine whether a similar mechanism operates during IC subtype specification in the kidney. One interpretation of this finding is that Notch activity is sequentially used in the INC lineage, first selecting out INC precursors, and then determining INC subtype, in much the same way that Notch is used at multiple steps during the diversification of cell types in the sensory organ precursor lineage in *Drosophila* (Cagan and Ready, 1989). The implication of this finding is that Notch activity regulates downstream targets expressed in INCs that then have a significant role in determining subtype identity.

ubp1, a member of the grainyhead transcription factor family, is one target in the skin that is regulated by Notch activity. Furthermore, we show that *ubp1* is expressed primarily in beta-INCs, suppresses the ability of foxi1 to activate the expression of *ae1* ectopically, and when misexpressed in embryos suppresses the formation of alpha-INCs and promotes the formation of beta-INCs. Significantly, ubp1 appears to execute a complete switch in subtype identity, by not only repressing the expression of *ae1*, but also by inducing *pendrin* and causing the H^+v-ATPase to localize basolaterally rather than apically. Attempts to substantiate these results further by inhibiting ubp1 activity using morpholinos have been unsuccessful, perhaps indicating that ubp1 overlaps in function with related members of the grainyhead family, cp2 and

cp2l1, both of which are also expressed in the skin (data not shown) (Hayes et al., 2007). Members of this grainyhead subfamily are known to heterodimerize and have been suggested to have overlapping functions (Yoon et al., 1994; Wilanowski et al., 2002; Sato et al., 2005; Katsura et al., 2009; To et al., 2010), although this has not been formally tested in vivo by making compound mutants. Thus, further work needs to be done to determine whether these grainyhead family members are indeed required for INC subtype specification by promoting the formation of beta-subtypes, or if ubp1 is acting fortuitously to regulate the expression of other transcription factors that normally serve this function.

Subtype specification is also altered, but in the opposite way, when INCs are induced by misexpression of foxi1-HGR. foxi1 induces an increase in both INC subtypes, but with a strong bias for alpha- over beta-INCs. The small increase in beta-INCs can be attributed to the observation that foxi1 also induces the expression of *ubp1* (I.K.Q., unpublished observations), perhaps explaining how expression of the subtype specification factors is initiated during INC formation. However, co-expression of *ubp1-HGR* along with *foxi-HGR* suppresses the formation of alpha-INCs while promoting beta-INC formation. Together, these results are best explained by a model in which the specification of INC subtypes is determined by the ratio between *ubp1*, acting as a beta-forming factor, and an unknown alpha-forming factor, the expression of which is activated by foxi1. A stochastic competition between these factors undergoing cross-repression would then act as a binary switch to ensure that the two subtypes form in a mutually exclusive manner but in a ratio determined, at least in part, by the levels of foxi1 and/or Notch activity. This model could explain why we have not detected INCs with a mixed subtype character, in which *pendrin* and *ae1* would be co-expressed, in any of the experimental manipulations described here, and why other studies have failed to show colocalization of ae1 and pendrin in any individual ICs in the kidney (Royaux et al., 2001; Song et al., 2007). The model also predicts the existence of an as yet unknown factor that is influenced by Notch and promotes the alpha-INC fate at the expense of beta-INCs by repressing *pendrin* expression and apical localization of the H^+v-ATPase.

Note added in proof

Dubaissi and Papalopulu (Dubaissi and Papalopulu, 2010) have recently described ionocytes in the *Xenopus* skin, focusing on the interaction of these cells with ciliated cells.

Acknowledgements

This work was supported by a grant (C.K.) from the NIH (GM07650). The AE1 monoclonal antibody developed by M. Jennings was obtained from the Developmental Studies Hybridoma Bank under the auspices of the NICHD and maintained by the University of Iowa (Department of Biology, Iowa City, IA 52242, USA. The authors thank Dr Nancy Papalopulu for communicating results prior to publication and Dr Ray Engeszer for helpful discussions. Deposited in PMC for release after 12 months.

Competing interests statement

The authors declare no competing financial interests.

Supplementary material

Supplementary material for this article is available at
http://dev.biologists.org/lookup/suppl/doi:10.1242/dev.055699/-/DC1

References

Al-Awqati, Q. (1996). Plasticity in epithelial polarity of renal intercalated cells: targeting of the H(+)-ATPase and band 3. *Am. J. Physiol.* **270**, C1571-C1580.
Amaya, E. and Kroll, K. L. (1999). A method for generating transgenic frog embryos. *Methods Mol. Biol.* **97**, 393-414.
Billett, F. S. and Gould, R. P. (1971). Fine structural changes in the differentiating epidermis of Xenopus laevis embryos. *J. Anat.* **108**, 465-480.
Blomqvist, S. R., Vidarsson, H., Fitzgerald, S., Johansson, B. R., Ollerstam, A., Brown, R., Persson, A. E., Bergstrom, G. G. and Enerback, S. (2004). Distal renal tubular acidosis in mice that lack the forkhead transcription factor Foxi1. *J. Clin. Invest.* **113**, 1560-1570.
Blomqvist, S. R., Vidarsson, H., Soder, O. and Enerback, S. (2006). Epididymal expression of the forkhead transcription factor Foxi1 is required for male fertility. *EMBO J.* **25**, 4131-4141.
Brend, T. and Holley, S. A. (2009). Zebrafish whole mount high-resolution double fluorescent in situ hybridization. *J. Vis. Exp*. pii 1229. doi: 10.3791/1229.
Breton, S. (2001). The cellular physiology of carbonic anhydrases. *JOP* **2**, 159-164.
Breton, S. and Brown, D. (2007). New insights into the regulation of V-ATPase-dependent proton secretion. *Am. J. Physiol. Renal Physiol.* **292**, F1-F10.
Brown, D. and Breton, S. (1996). Mitochondria-rich, proton-secreting epithelial cells. *J. Exp. Biol.* **199**, 2345-2358.
Cagan, R. L. and Ready, D. F. (1989). Notch is required for successive cell decisions in the developing Drosophila retina. *Genes Dev.* **3**, 1099-1112.
Davidson, L. A., Hoffstrom, B. G., Keller, R. and DeSimone, D. W. (2002). Mesendoderm extension and mantle closure in Xenopus laevis gastrulation: combined roles for integrin alpha(5)beta(1), fibronectin, and tissue geometry. *Dev. Biol.* **242**, 109-129.
Devonald, M. A., Smith, A. N., Poon, J. P., Ihrke, G. and Karet, F. E. (2003). Non-polarized targeting of AE1 causes autosomal dominant distal renal tubular acidosis. *Nat. Genet.* **33**, 125-127.
Dubaissi, E. and Papalopulu, P. (2010). Embryonic frog epidermis: a model for the study of cell-cell interactions in the development of mucociliary disease. *Dis. Model. Mech*. Published online ahead of print December 23, 2010, doi:10.1242/dmm006494.
Ehrenfeld, J. and Klein, U. (1997). The key role of the H+ V-ATPase in acid-base balance and Na+ transport processes in frog skin. *J. Exp. Biol.* **200**, 247-256.
Fryer, C. J., Lamar, E., Turbachova, I., Kintner, C. and Jones, K. A. (2002). Mastermind mediates chromatin-specific transcription and turnover of the Notch enhancer complex. *Genes Dev.* **16**, 1397-1411.
Gao, X., Eladari, D., Leviel, F., Tew, B. Y., Miró-Julià, C., Cheema, F., Miller, L., Nelson, R., Paunescu, T. G., McKee, M. et al. (2010). Deletion of hensin/DMBT1 blocks conversion of β- to α-intercalated cells and induces distal renal tubular acidosis. *Proc. Natl. Acad. Sci. USA* **107**, 21872-21877.
Harland, R. M. (1991). In situ hybridization: an improved whole-mount method for Xenopus embryos. *Methods Cell Biol.* **36**, 685-695.
Hayes, J. M., Kim, S. K., Abitua, P. B., Park, T. J., Herrington, E. R., Kitayama, A., Grow, M. W., Ueno, N. and Wallingford, J. B. (2007). Identification of novel ciliogenesis factors using a new in vivo model for mucociliary epithelial development. *Dev. Biol.* **312**, 115-130.
Heasman, J. (2002). Morpholino oligos: making sense of antisense? *Dev. Biol.* **243**, 209-214.
Hiatt, M. J., Ivanova, L., Toran, N., Tarantal, A. F. and Matsell, D. G. (2010). Remodeling of the fetal collecting duct epithelium. *Am. J. Pathol.* **176**, 630-637.
Hinton, A., Bond, S. and Forgac, M. (2009). V-ATPase functions in normal and disease processes. *Pflugers Arch.* **457**, 589-598.
Hsiao, C. D., You, M. S., Guh, Y. J., Ma, M., Jiang, Y. J. and Hwang, P. P. (2007). A positive regulatory loop between foxi3a and foxi3b is essential for specification and differentiation of zebrafish epidermal ionocytes. *PLoS One* **2**, e302.
Hulander, M., Kiernan, A. E., Blomqvist, S. R., Carlsson, P., Samuelsson, E. J., Johansson, B. R., Steel, K. P. and Enerback, S. (2003). Lack of pendrin expression leads to deafness and expansion of the endolymphatic compartment in inner ears of Foxi1 null mutant mice. *Development* **130**, 2013-2025.
Hwang, P. P. and Lee, T. H. (2007). New insights into fish ion regulation and mitochondrion-rich cells. *Comp. Biochem. Physiol. A Mol. Integr. Physiol.* **148**, 479-497.
Janicke, M., Carney, T. J. and Hammerschmidt, M. (2007). Foxi3 transcription factors and Notch signaling control the formation of skin ionocytes from epidermal precursors of the zebrafish embryo. *Dev. Biol.* **307**, 258-271.
Janicke, M., Renisch, B. and Hammerschmidt, M. (2010). Zebrafish grainyhead-like1 is a common marker of different non-keratinocyte epidermal cell lineages, which segregate from each other in a Foxi3-dependent manner. *Int. J. Dev. Biol.* **54**, 837-850.
Jensen, L. J., Willumsen, N. J. and Larsen, E. H. (2002). Proton pump activity is required for active uptake of chloride in isolated amphibian skin exposed to freshwater. *J. Comp. Physiol. B* **172**, 503-511.
Jensen, L. J., Willumsen, N. J., Amstrup, J. and Larsen, E. H. (2003). Proton pump-driven cutaneous chloride uptake in anuran amphibia. *Biochim. Biophys. Acta* **1618**, 120-132.
Jeong, H. W., Jeon, U. S., Koo, B. K., Kim, W. Y., Im, S. K., Shin, J., Cho, Y., Kim, J. and Kong, Y. Y. (2009). Inactivation of Notch signaling in the renal collecting duct causes nephrogenic diabetes insipidus in mice. *J. Clin. Invest.* **119**, 3290-3300.
Karet, F. E., Finberg, K. E., Nelson, R. D., Nayir, A., Mocan, H., Sanjad, S. A., Rodriguez-Soriano, J., Santos, F., Cremers, C. W., Di Pietro, A. et al. (1999).

Mutations in the gene encoding B1 subunit of H+-ATPase cause renal tubular acidosis with sensorineural deafness. *Nat. Genet.* **21**, 84-90.
Katsura, A., Kimura, K., Hosoi, K., Tomokuni, Y., Nesori, M., Goryo, K., Numayama-Tsuruta, K., Torii, S., Yasumoto, K., Gotoh, O. et al. (2009). Transactivation activity of LBP-1 proteins and their dimerization in living cells. *Genes Cells* **14**, 1183-1196.
Kim, Y. H., Kwon, T. H., Frische, S., Kim, J., Tisher, C. C., Madsen, K. M. and Nielsen, S. (2002). Immunocytochemical localization of pendrin in intercalated cell subtypes in rat and mouse kidney. *Am. J. Physiol. Renal Physiol.* **283**, F744-F754.
Klein, U., Timme, M., Zeiske, W. and Ehrenfeld, J. (1997). The H+ pump in frog skin (Rana esculenta): identification and localization of a V-ATPase. *J. Membr. Biol.* **157**, 117-126.
Kobayashi, K., Uchida, S., Mizutani, S., Sasaki, S. and Marumo, F. (2001). Intrarenal and cellular localization of CLC-K2 protein in the mouse kidney. *J. Am. Soc. Nephrol.* **12**, 1327-1334.
Kolm, P. J. and Sive, H. L. (1995). Efficient hormone-inducible protein function in Xenopus laevis. *Dev. Biol.* **171**, 267-272.
Krogh, A. (1937). Osmotic regulation in the frog (R. esculenta) by active absorption of chloride ions. *Skand. Arch. Physiol.* **71**, 60-73.
Krogh, A. (1938). The active absorption of ions in some fresh water animals. *Z. Vgl. Physiol.* **25**, 335-350.
Kujala, M., Hihnala, S., Tienari, J., Kaunisto, K., Hastbacka, J., Holmberg, C., Kere, J. and Hoglund, P. (2007). Expression of ion transport-associated proteins in human efferent and epididymal ducts. *Reproduction* **133**, 775-784.
Larsen, E. H., Christoffersen, B. C., Jensen, L. J., Sorensen, J. B. and Willumsen, N. J. (1996). Role of mitochondria-rich cells in epithelial chloride uptake. *Exp. Physiol.* **81**, 525-534.
Mir, A., Kofron, M., Zorn, A. M., Bajzer, M., Haque, M., Heasman, J. and Wylie, C. C. (2007). FoxI1e activates ectoderm formation and controls cell position in the Xenopus blastula. *Development* **134**, 779-788.
Mir, A., Kofron, M., Heasman, J., Mogle, M., Lang, S., Birsoy, B. and Wylie, C. (2008). Long- and short-range signals control the dynamic expression of an animal hemisphere-specific gene in Xenopus. *Dev. Biol.* **315**, 161-172.
Oliver, J. (1944). New directions for renal morphology: a method, its results and its future. *The Harvey Lectures*, Ser XL 102-155.
Parekh, V., McEwen, A., Barbour, V., Takahashi, Y., Rehg, J. E., Jane, S. M. and Cunningham, J. M. (2004). Defective extraembryonic angiogenesis in mice lacking LBP-1a, a member of the grainyhead family of transcription factors. *Mol. Cell. Biol.* **24**, 7113-7129.
Pietrement, C., Sun-Wada, G. H., Silva, N. D., McKee, M., Marshansky, V., Brown, D., Futai, M. and Breton, S. (2006). Distinct expression patterns of different subunit isoforms of the V-ATPase in the rat epididymis. *Biol. Reprod.* **74**, 185-194.
Royaux, I. E., Wall, S. M., Karniski, L. P., Everett, L. A., Suzuki, K., Knepper, M. A. and Green, E. D. (2001). Pendrin, encoded by the Pendred syndrome gene, resides in the apical region of renal intercalated cells and mediates bicarbonate secretion. *Proc. Natl. Acad. Sci. USA* **98**, 4221-4226.
Sakamoto, H., Sado, Y., Naito, I., Kwon, T. H., Inoue, S., Endo, K., Kawasaki, M., Uchida, S., Nielsen, S., Sasaki, S. et al. (1999). Cellular and subcellular immunolocalization of ClC-5 channel in mouse kidney: colocalization with H+-ATPase. *Am. J. Physiol.* **277**, F957-F965.
Sato, F., Yasumoto, K., Kimura, K., Numayama-Tsuruta, K. and Sogawa, K. (2005). Heterodimerization with LBP-1b is necessary for nuclear localization of LBP-1a and LBP-1c. *Genes Cells* **10**, 861-870.
Schachowa, S. (1876). *Untersuchungen uber die Niere*. Medical thesis dissertation. Berne, Switzerland.
Schiefferdecker, P. (1881). Zur Kenntis des Baues der Schleimdrusen. *Arch. Mikrosk. Anat.* **23**, 382-412.
Schulz, N., Dave, M. H., Stehberger, P. A., Chau, T. and Wagner, C. A. (2007). Differential localization of vacuolar H+-ATPases containing a1, a2, a3, or a4 (ATP6V0A1-4) subunit isoforms along the nephron. *Cell. Physiol. Biochem.* **20**, 109-120.
Schulze, F. E. (1876). Epithel- und Drusen-Zellen. *Arch. Mikrosk. Anat.* **3**, 137-203.
Schwartz, G. J. and Al-Awqati, Q. (2005). Role of hensin in mediating the adaptation of the cortical collecting duct to metabolic acidosis. *Curr. Opin. Nephrol. Hypertens.* **14**, 383-388.
Schwartz, G. J., Tsuruoka, S., Vijayakumar, S., Petrovic, S., Mian, A. and Al-Awqati, Q. (2002). Acid incubation reverses the polarity of intercalated cell transporters, an effect mediated by hensin. *J. Clin. Invest.* **109**, 89-99.
Sive, H., Grainger, R. M. and Harland, R. M. (1998). *The Early Development of Xenopus laevis: A Laboratory Manual*. Plainview, NY: Cold Spring Harbor Laboratory Press.
Song, H. K., Kim, W. Y., Lee, H. W., Park, E. Y., Han, K. H., Nielsen, S., Madsen, K. M. and Kim, J. (2007). Origin and fate of pendrin-positive intercalated cells in developing mouse kidney. *J. Am. Soc. Nephrol.* **18**, 2672-2682.
Sparrow, D. B., Latinkic, B. and Mohun, T. J. (2000). A simplified method of generating transgenic Xenopus. *Nucleic Acids Res.* **28**, E12.
Stehberger, P. A., Schulz, N., Finberg, K. E., Karet, F. E., Giebisch, G., Lifton, R. P., Geibel, J. P. and Wagner, C. A. (2003). Localization and regulation of the ATP6V0A4 (a4) vacuolar H+-ATPase subunit defective in an inherited form of distal renal tubular acidosis. *J. Am. Soc. Nephrol.* **14**, 3027-3038.
Stehberger, P. A., Shmukler, B. E., Stuart-Tilley, A. K., Peters, L. L., Alper, S. L. and Wagner, C. A. (2007). Distal renal tubular acidosis in mice lacking the AE1 (band3) Cl-/HCO3- exchanger (slc4a1). *J. Am. Soc. Nephrol.* **18**, 1408-1418.
Stubbs, J. L., Davidson, L., Keller, R. and Kintner, C. (2006). Radial intercalation of ciliated cells during Xenopus skin development. *Development* **133**, 2507-2515.
Suri, C., Haremaki, T. and Weinstein, D. C. (2005). Xema, a foxi-class gene expressed in the gastrula stage Xenopus ectoderm, is required for the suppression of mesendoderm. *Development* **132**, 2733-2742.
To, S., Rodda, S. J., Rathjen, P. D. and Keough, R. A. (2010). Modulation of CP2 family transcriptional activity by CRTR-1 and sumoylation. *PLoS One* **5**, e11702.
Vidarsson, H., Westergren, R., Heglind, M., Blomqvist, S. R., Breton, S. and Enerback, S. (2009). The forkhead transcription factor Foxi1 is a master regulator of vacuolar H-ATPase proton pump subunits in the inner ear, kidney and epididymis. *PLoS One* **4**, e4471.
Wagner, C. A., Finberg, K. E., Stehberger, P. A., Lifton, R. P., Giebisch, G. H., Aronson, P. S. and Geibel, J. P. (2002). Regulation of the expression of the Cl^-/anion exchanger pendrin in mouse kidney by acid-base status. *Kidney Int.* **62**, 2109-2117.
Wagner, C. A., Finberg, K. E., Breton, S., Marshansky, V., Brown, D. and Geibel, J. P. (2004). Renal vacuolar H+-ATPase. *Physiol. Rev.* **84**, 1263-1314.
Wagner, C. A., Devuyst, O., Bourgeois, S. and Mohebbi, N. (2009). Regulated acid-base transport in the collecting duct. *Pflugers Arch.* **458**, 137-156.
Wall, S. M. (2005). Recent advances in our understanding of intercalated cells. *Curr. Opin. Nephrol. Hypertens.* **14**, 480-484.
Wettstein, D. A., Turner, D. L. and Kintner, C. (1997). The Xenopus homolog of Drosophila Suppressor of Hairless mediates Notch signaling during primary neurogenesis. *Development* **124**, 693-702.
Wilanowski, T., Tuckfield, A., Cerruti, L., O'Connell, S., Saint, R., Parekh, V., Tao, J., Cunningham, J. M. and Jane, S. M. (2002). A highly conserved novel family of mammalian developmental transcription factors related to Drosophila grainyhead. *Mech. Dev.* **114**, 37-50.
Yoon, J. B., Li, G. and Roeder, R. G. (1994). Characterization of a family of related cellular transcription factors which can modulate human immunodeficiency virus type 1 transcription in vitro. *Mol. Cell. Biol.* **14**, 1776-1785.
Zapala, M. A., Lockhart, D. J., Pankratz, D. G., Garcia, A. J. and Barlow, C. (2002). Software and methods for oligonucleotide and cDNA array data analysis. *Genome Biol.* **3**, SOFTWARE0001.